PHYSICAL REVIEW C VOLUME 57, NUMBER 2 FEBRUARY 1998

Dimensional effects in a relativistic mean-field approach

A. Delfino, Lizardo H. C. M. Nunes, and J. S. Sá Martins
Instituto de Física, Universidade Federal Fluminense, Avenida Litorânea s/n, 24210 340, Niterói, Rio de Janeiro, Brazil
(Received 15 October 1997)

We study the Walecka model in one and two spatial dimensions within a mean-field approach. Inspired by infinite nuclear matter, where this model is usually applied, we compare how the observables behave when their phase space is reduced. We find a closed and unified relativistic expression for the compression modulus as well as the relativistic expansion of the model, both dependent on dimension only. This relativistic expansion is analyzed regarding the saturation and/or collapse of the system. [S0556-2813(98)05302-3]

PACS number(s): 24.10.Jv, 24.10.Nz, 21.65.+f, 25.75.−q

I. INTRODUCTION

There is a large amount of literature showing that the reduction of the spatial dimension (three to one, for instance) may cause some many-body problems to have analytical solutions. The most classic example is the one-dimensional N body (boson) system interacting pairwise via a $-g\delta(x)$ attractive potential, where an exact analytical bound-state solution can be found through the many-body wave function given by the Bethe ansatz, showing that the binding energy of the system (in units of $\hbar=m=c=1$) is $E_N=-N(N^2-1)g^2/24$ [1]. A mean-field approximation for the same system has been found giving $E_N=-N(N-1)^2g^2/24$ [2]. Both solutions agree to leading order in N, exhibiting the expected behavior for the mean-field approximation, which turns out to be improved as the density of the system increases.

Another feature of this one-dimensional system is that the bound-state energy per particle does not saturate, as $N\rightarrow\infty$. Idealized one-dimensional systems are rich in providing many simplified results for bound and scattering states, see for instance Refs. [2–4].

The underlying physics coming from phase space of different dimensionalities starts to appear already in the quantum-mechanical two-body problem. If there is any attractive interaction, at least one bound state exists for a two-body system in one dimension. For two and three dimensions the possibility of two-body binding depends on the strength and/or range of the interaction. Some typical nonrelativistic three-body effects also depend on the dimension of phase space. This is the situation in the Thomas and Efimov effects [5,6]. The first one shows the following. Suppose one has a system of three bosons interacting via a short-range (r_0) two-body interaction $\lambda V(r)$. If r_0 approaches zero while λ is increased such that the two-body binding energy is kept fixed, then the three-body binding energy diverges. On the other hand, the Efimov effect shows that if three nonrelativistic identical bosons interact via a short-range two-particle interaction $\lambda V(r)$, characterized by a range parameter r_0, then in the limit $\lambda\rightarrow\lambda_0$, where λ_0 is the strength needed to support the first zero-energy two-particle bound state, the number of three-particle s-wave bound states approaches infinity. These two apparently distinct effects are essentially related to the same mechanism (divergence of the trace of the kernel of the three-particle system scattering equation), and do not exist in one and two dimensions [7].

Relativistic corrections and/or the assumption of fermionic character of the particles in the system may substantially alter the results obtained for nonrelativistic bosonic systems. For example, if one treats relativistically the three-body problem with zero-range interactions, the Thomas effect does not arise [8]. It is also reasonable to expect that, even in a nonrelativistic approach, the Pauli principle would help to prevent collapsing systems. Dimensionality effects on hadronic matter calculations regarding correlation functions [9] and dibaryon condensates in nuclear matter [10] have recently been reported.

Ground-state properties in a model quantum field theory have been calculated in one spatial dimension [11], looking for stochastic solutions. The model consisted of nonrelativistic nucleons coupled to vector and scalar mesons. The aim of that work was to open the way for more involved real calculations in three spatial dimensions. Here, we intend to exploit the model in its relativistic context for one and two spatial dimensions, studying ground-state properties and connecting these to the three-dimensional case. Motivated by current applications of the Walecka model [12] to nuclear matter, we assume each spatial case to saturate the infinite nuclear matter at the same values as its three-dimensional counterpart. We have obtained a relativistic closed unified expression for the compression modulus in one, two, and three spatial dimensions.

After having compared the model in different spacial dimensions in the full relativistic calculation, we perform a relativistic expansion in powers of the Fermi momenta, in order to study the impact of relativistic corrections. A closed and unified expansion depending only on the dimensionality is achieved. As a particular case, we have taken the nonrelativistic limit to conclude that, in one dimension, this model saturates the infinite nuclear matter (in accordance with Ref. [11]), whereas in two and three spatial dimensions it predicts the system's collapse. Following the relativistic expansion, we have verified that, for all dimensionalities, the first order of relativistic correction can avoid collapse.

The outline of this paper is as follows. In Sec. II we present the model and in Sec. III we discuss the relativistic expansion for the model, which is presented in more detail in the Appendix. In Sec. IV we present our results, and our conclusions are given in Sec. V.

II. THE MODEL

The model we deal with is presented in detail in Ref. [12]. The degrees of freedom are baryon fields (ψ), scalar meson fields (σ), and vector meson fields (ω). The Lagrangian density is given by

$$\mathcal{L}_W=\overline{\psi i}\gamma_\mu\partial^\mu\psi-\overline{\psi}M\psi+\frac{1}{2}(\partial_\mu\sigma\partial^\mu\sigma-m_s^2\sigma^2)+g_s\sigma\overline{\psi}\psi$$
$$-\frac{1}{4}F^{\mu\nu}F_{\mu\nu}+\frac{1}{2}m_v^2\omega_\mu\omega^\mu-g_v\overline{\psi}\gamma_\mu\psi\omega^\mu, \tag{1}$$

where $F_{\mu\nu}=\partial_\mu\omega_\nu-\partial_\nu\omega_\mu$, M is the bare nucleon mass, and m_s and m_v are the scalar and vector mesonic masses respectively. Since we intend to apply this Lagrangian to space dimensionalities $D=3$ (3D), $D=2$ (2D) and $D=1$ (1D), let us establish the dimensions of the fields and coupling constants. In units of the baryonic mass M, $[\psi]\equiv M^{D/2}$, $[\sigma]\equiv M^{(D-1)/2}$, and $[g_s]\equiv M^{(3-D)/2}$. The vector field and the vector-baryonic coupling constant have the same dimension as the scalar one.

Now we pursue a common approach to the different dimensions, until phase space dimensionality manifests itself explicitly and separates the various cases. From the above Lagrangian we obtain, through the Euler-Lagrange formalism, the equations of motion for the nucleon and mesons fields:

$$[i\gamma_\mu\partial^\mu-(M-g_s\sigma)-g_v\gamma_\mu\omega^\mu]\psi=0, \tag{2}$$

$$\partial_\nu F^{\nu\mu}+m_v^2\omega^\mu=g_v\overline{\psi}\gamma^\mu\psi, \tag{3}$$

$$(\partial_\mu\partial^\mu+m_s^2)\sigma=g_s\overline{\psi}\psi. \tag{4}$$

When the meson fields are replaced by the constant classical fields σ_0 and ω_0, we arrive at the mean-field approximation with the equations

$$\omega_0=\frac{g_\omega}{m_v^2}\langle\psi^+\psi\rangle=\frac{g_v}{m_\omega^2}\rho_b, \tag{5}$$

$$\sigma_0=\frac{g_s}{m_\sigma^2}\langle\overline{\psi}\psi\rangle, \tag{6}$$

The constant classical fields σ_0 and ω_0 are thus directly related to the baryon sources. The source for ω_0 is simply the baryon density $\rho_b=N/V$ (hereafter referred to as ρ) which is a constant of the motion for a uniform system of N baryons in a volume V. The source for σ_0 involves the expectation value of the Lorentz scalar density $\overline{\psi}\psi=\rho_s$.

Now we define the scalar (S) and the vector (V) potentials. This can be done by looking at the Dirac equation for the models, Eq. (2), and rewriting M^* in the form $M^*=M-g_s\sigma=M+S$. Still from the analysis of the Dirac equation, V can be defined as a quantity which shifts the energy, $V=g_v\omega_0$.

It is convenient to introduce the following dimensionless quantities $y=M^*/M$, $C_s^2=g_s^2M^{D-1}/m_s^2$, and $C_v^2=g_v^2M^{D-1}/m_v^2$, as well as some auxiliary field densities:

$$\mathcal{E}_\omega=\frac{C_v^2}{2M^{(D-1)}}\rho^2, \tag{7}$$

$$\mathcal{E}_\sigma=\frac{M^{(D+1)}}{2C_s^2}(1-y)^2, \tag{8}$$

$$\mathcal{E}_b=\gamma\Lambda_D\int d^DkE^*(k)(n_k+\overline{n_k}), \tag{9}$$

$$p_b=\frac{1}{D}\gamma\Lambda_D\int d^Dk\,\frac{k^2}{E^*(k)}(n_k+\overline{n_k}), \tag{10}$$

$$\rho=\gamma\Lambda_D\int d^DkE^*(k)(n_k-\overline{n_k}). \tag{11}$$

In these expressions, γ is the degeneracy factor ($\gamma=4$ for nuclear matter and $\gamma=2$ for neutron matter), n_k and $\overline{n_k}$ stand for the Fermi-Dirac distribution for baryons and antibaryons, respectively, with arguments $(E^*-\nu)/T$. $E^*(k)$ is given by $E^*(k)=(k^2+M^{*2})^{(1/2)}$, whereas an effective chemical potential, which preserves the number of baryons and antibaryons in the ensemble, is defined by $\nu=\mu-V$, where μ is the thermodynamic chemical potential. Λ_D is the volume of the elementary cell in D-dimensional phase space, $(\pi)^{-D}$. In the zero temperature limit, the ground state is obtained by filling energy levels up to a Fermi surface k_f, and thus n_k approaches $\Theta(k_f-k)$ and $\overline{n_k}$ vanishes.

The expressions for the energy density and pressure can be found, as usual, by averaging the energy-momentum tensor, and can be presented in terms of the above quantities as

$$\mathcal{E}=\mathcal{E}_\omega+\mathcal{E}_\sigma+\mathcal{E}_b, \tag{12}$$

and

$$p=\mathcal{E}_\omega-\mathcal{E}_\sigma+p_b. \tag{13}$$

The solution for the equation of state is obtained explicitly through the minimization of $\mathcal{E}$ relative to the scalar field, or equivalently y. This equation (known as the gap equation) has to be solved self-consistently and provides the basis for obtaining all thermodynamic quantities in the mean field approach we are using. In a general way, it reads

$$1-y-\frac{C_s^2}{M^D}\rho_s=0. \tag{14}$$

Note that $\rho_s=\langle\overline{\psi}\psi\rangle$, $\mathcal{E}_b$, p_b and ρ have D as a parameter, in a way to be made explicit in the following. Defining new dimensionless variables $x=k/M$ and $e^*(x)=(x^2+y^2)^{(1/2)}$, the densities for different spatial dimensions are as follows.

3D:

$$\rho=\frac{\gamma M^3}{6\pi^2}x_f^3, \tag{15}$$

$$\rho_s=\frac{\gamma M^3y}{4\pi^2}\left[x_fe_f-y^2\ \ln\frac{x_f+e_f}{y}\right], \tag{16}$$

$$\mathcal{E}_b=\frac{\gamma M^4}{8\pi^2}\left[x_f e_f^3-\frac{y^2}{2}x_f e_f-\frac{y^4}{2}\ln\frac{x_f+e_f}{y}\right], \tag{17}$$

$$p_b=\frac{\gamma M^4}{6\pi^2}\left[x_f^3 e_f-\frac{3}{4}x_f e_f^3+\frac{3}{8}y^2 x_f e_f+\frac{3y^4}{8}\ln\frac{x_f+e_f}{y}\right], \tag{18}$$

2D:

$$\rho=\frac{\gamma M^2}{4\pi}x_f^2, \tag{19}$$

$$\rho_s=\frac{\gamma M^2}{2\pi}[e_f-y]y, \tag{20}$$

$$\mathcal{E}_b=\frac{\gamma M^3}{2\pi}\left[\frac{1}{3}e_f^3-\frac{y^3}{3}\right], \tag{21}$$

$$p_b=\frac{\gamma M^3}{2\pi}\left[\frac{e_f^3}{6}+\frac{y^3}{3}-\frac{1}{2}y^2 e_f\right]. \tag{22}$$

1D:

$$\rho=\frac{\gamma M}{\pi}x_f, \tag{23}$$

$$\rho_s=\frac{\gamma M}{\pi}y\,\ln\frac{x_f+e_f}{y}, \tag{24}$$

$$\mathcal{E}_b=\frac{\gamma M^2}{2\pi}\left[x_f e_f+y^2\,\ln\frac{x_f+e_f}{y}\right], \tag{25}$$

$$p_b=\frac{\gamma M^2}{2\pi}\left[x_f e_f-y^2\,\ln\frac{x_f+e_f}{y}\right]. \tag{26}$$

The free baryonic densities have to be added to the mesonic scalar densities [Eqs. (7), (8)] in order to obtain the equation of state (EOS) Eqs. (12), (13). The baryonic scalar density ρ_s has to be inserted into Eq. (14) to obtain the effective baryonic mass solutions. Having completely specified the model, we are in a position to calculate the EOS for all cases. Once Eq. (14) is solved for any k_f, the value of y has to be substituted into Eqs. (12), (13). The dimensionless coupling constants $C_s^2=g_s^2M^{D-1}/m_s^2$ and $C_v^2=g_v^2M^{D-1}/m_v^2$ can be eliminated in favor of the experimental values $\mathcal{E}/\rho_0-M=-16$ MeV, where ρ_0 is fixed by $k_f=1.3\ \text{fm}^{-1}$. Note that the mean field approach reduces the number of free parameters we have started with in our Lagrangian, Eq. (1), for all spatial dimensions. Instead of four, they are only two, C_s^2 and C_v^2, uniquely determined by the above-imposed constraint.

Now, we present two interesting features of our study. First, the compression modulus can be put into a unified closed form. The compression modulus K is defined [15] by

$$K=k_f^2\frac{\partial^2}{\partial k_f^2}\left(\frac{\mathcal{E}}{\rho}\right)\bigg|_{k_f=k_f^0}. \tag{27}$$

Using the relations between k_f and ρ for the different dimensionalities above, K can be rewritten as

$$K=D^2\frac{\partial}{\partial\rho}p|_{\rho=\rho_0}, \tag{28}$$

or equivalently, in a way more suitable for our purposes,

$$K=D^2\left[-\frac{\mathcal{E}+p}{\rho}+\frac{\partial}{\partial\rho}(\mathcal{E}+p)\right]\bigg|_{\rho=\rho_0}. \tag{29}$$

After a trivial but tedious rearranging of terms, we end up with

$$K=\left(\frac{D^2C_v^2}{M^{D-1}}\right)\rho_0+DM\left(\frac{x_f^2}{e_f}\right)-\left(\frac{C_s^2D^2}{M^{D-1}}\right)\times\left(\frac{y^2}{e_f^2}\right)\frac{\rho}{1+(C_s^2D/M^D)(\rho_s/y-\rho/e_f)}, \tag{30}$$

which in 3D agrees with previous results [14]. Second, the two-dimensional case reduces the gap equation [Eq. (14)] to a cubic one in y:

$$1-y-a[(x_f^2+y^2)^{1/2}-y]y=0, \tag{31}$$

where we have defined $a=\gamma C_s^2/2\pi$. This equation allows an algebraic solution for y instead of the transcendental equations for the 3D and 1D cases. However, the complete determination of y, with the elimination of C_s^2 and C_v^2 by imposing $B_0=\mathcal{E}/\rho_0-M$ for a given equilibrium density ρ_0, leads to a sixth-order algebraic equation for y, without a visible practical advantage relative to a direct standard numerical solution. Nonetheless this 2D case exhibits the interesting aspect of having an analytic solution for the model.

III. RELATIVISTIC EXPANSIONS

In this section, we analyze the relativistic expansion for the models. We start performing a M^* expansion in powers of k_f iteratively in Eq. (14) and substituting these values into Eqs. (12), (13). By so doing, we intend to see whether the nonrelativistic limit of the model ensures saturation, as well as how sizable the first relativistic correction is.

The relativistic expansion is based on the series development of $(k_f^2+M^{*2})^{1/2}$, where the expansion parameter k_f^2/M^{*2} is assumed to be smaller than one. It turns out that the expansion for the equation of state can be presented in a unified form:

$$M^*=M-\frac{\rho C_s^2}{M^{(D-1)}}\sum_{n=0}^{\infty}\frac{D}{D+2n}B_n\frac{k_f^{2n}}{M^{*(2n)}}, \tag{32}$$

$$\mathcal{E}=\frac{C_v^2}{2M^{(D-1)}}\rho^2+\frac{C_s^2}{2M^{(D-1)}}\rho^2\left[\sum_{n=0}^{\infty}\frac{D}{D+2n}B_n\frac{k_f^{2n}}{M^{*(2n)}}\right]^2+\rho\sum_{n=0}^{\infty}\frac{D}{D+2n}C_n\frac{k_f^{2n}}{M^{*(2n-1)}}, \tag{33}$$

$$p=\frac{C_v^2}{2M^{(D-1)}}\rho^2-\frac{C_s^2}{2M^{(D-1)}}\rho^2\left[\sum_{n=0}^{\infty}\frac{D}{D+2n}B_n\frac{k_f^{2n}}{M^{*(2n)}}\right]^2+\frac{\rho k_f^2}{M^*}\sum_{n=0}^{\infty}\frac{B_n}{D+2(n+1)}\frac{k_f^{2n}}{M^{*(2n)}}, \tag{34}$$

where

$$B_n=\binom{-1/2}{n},\quad C_n=\binom{1/2}{n} \tag{35}$$

and D is the dimensional case 1, 2, or 3. By using the relationship $C_{n+1}=B_n/2(n+1)$ it is easy to show that the above expansions satisfy the relation $(\mathcal{E}+p)/\rho=\mu$, showing the consistency of the relativistic expansion with the Hugenholtz–van Hove theorem [16] at each order of k_f. In fact, Boguta [17] found it surprising that this theorem, proved for the exact solution of the many-body problem, was still valid in the Hartree approximation. Here we verified that this result is also valid in the mean field approach, at each order of its relativistic expansion.

Equations (32)–(34) are still functions of M^*, which is the solution to be sought from Eq. (32). In order to proceed to a more palatable expansion, one needs the expansion of M^* iteratively in terms of M at the desirable power of k_f to expand the Eqs. (33), (34) also in terms of M. This procedure leads to more insight on aspects of the expansion itself. We illustrate this in the Appendix. Following the interpretation of Forest and Pandharipande [13], the first row of Eqs. (A2), (A5), and (A8), without the last grouped term, are nonrelativistic contributions to the binding energy. The second row gives the relativistic correction to the kinetic energy of a Fermi gas and all the subsequent terms in those expansions are relativistic corrections to the interaction energy.

To begin with, let us keep only the lower order nonrelativistic terms (nonrelativistic Fermi kinetic energy plus the interacting mesonic term),
3D:

$$\frac{\mathcal{E}}{\rho}-M=\left(\frac{3}{10M}\right)\left(\frac{6\pi^2\rho}{\gamma}\right)^{2/3}+\left(\frac{C_v^2-C_s^2}{2M^2}\right)\rho; \tag{36}$$

2D:

$$\frac{\mathcal{E}}{\rho}-M=\left(\frac{\pi}{\gamma M}\right)\rho+\left(\frac{C_v^2-C_s^2}{2M}\right)\rho; \tag{37}$$

1D:

$$\frac{\mathcal{E}}{\rho}-M=\left(\frac{\pi^2}{6\gamma^2 M}\right)\rho^2+\left(\frac{C_v^2-C_s^2}{2}\right)\rho. \tag{38}$$

It is easy to conclude from these expressions that, in the nonrelativistic limit, 1D allows saturation, since $C_s^2>C_v^2$ (in agreement with Ref. [11]), whereas 3D and 2D predict collapsing systems as ρ increases.

The 1D nonrelativistic saturation deserves a comment. As can be seen from Eq. (38), differently from the relativistic cases presented before, there are now no longer two free parameters. The difference $(C_v^2-C_s^2)$ works as the only free parameter in the model and we cannot specify them separately in a unique way. Suppose we have to adjust the binding energy per particle B_0 at a certain density ρ_0. Minimizing $\mathcal{E}/\rho$ relative to ρ in Eq. (38), we obtain

$$\rho_0=\frac{3\gamma^2 M}{2\pi^2}(C_s^2-C_v^2); \tag{39}$$

by plugging back this value of ρ_0 into Eq. (38), we have

$$C_s^2-C_v^2=\left(\frac{8B_0\pi^2}{3\gamma^2 M}\right)^{1/2}, \tag{40}$$

and therefore both constants are determined in terms of only one observable ρ_0 or B_0. If we then choose to eliminate these parameters in favor of B_0, for example, the density becomes completely determined by the binding energy

$$\rho_0=\left(\frac{6\gamma^2 M B_0}{\pi^2}\right)^{1/2}. \tag{41}$$

It is interesting to see that in this way, the compression modulus is also given by the fixed binding energy

$$K=2B_0. \tag{42}$$

As a last remark on this nonrelativistic case, we point out that Eq. (38) is equivalent to the first-order energy expansion (direct term, without exchange) for an infinite Fermi gas interacting via a pairwise $-g\delta(x)$ potential, with g directly related to $(C_v^2-C_s^2)$. It is also clear from this equation that the system is allowed to saturate due only to kinetic energy, without any need for the repulsive interaction.

The simple inclusion of nonrelativistic higher-order terms from Eqs. (A2), (A5), and (A8), without inclusion of the corresponding order from the relativistic contribution (second row of those equations), may be misleading, and therefore we proceed to take consistently the lowest order relativistic correction to the model,
3D:

$$\frac{\mathcal{E}}{\rho}-M=\left(\frac{C_v^2-C_s^2}{2M^2}\right)\rho+\frac{3}{10}\frac{k_f^2}{M}-\frac{3}{56}\frac{k_f^4}{M^3}+C_s^2\frac{\rho}{M}\frac{3}{10}\frac{k_f^2}{M}, \tag{43}$$

$$p=\left(\frac{C_v^2-C_s^2}{2M^2}\right)\rho^2+\frac{1}{5}\frac{k_f^2}{M}\rho-\frac{1}{14}\frac{k_f^4}{M^3}\rho+C_s^2\frac{\rho^2}{M^2}\frac{3}{10}\frac{k_f^2}{4M^2}, \tag{44}$$

$$M^*=M-C_s^2\frac{\rho}{M^2}\left(1-\frac{3}{10}\frac{k_f^2}{M^2}\right), \tag{45}$$

2D:

$$\frac{\mathcal{E}}{\rho}-M=\left(\frac{C_v^2-C_s^2}{2M^2}\right)\rho+\frac{1}{4}\frac{k_f^2}{M}-\frac{1}{24}\frac{k_f^4}{M^3}+C_s^2\frac{\rho}{M}\frac{1}{4}\frac{k_f^2}{M}, \tag{46}$$

$$p=\left(\frac{C_v^2-C_s^2}{2M^2}\right)\rho^2+\frac{1}{4}\frac{k_f^2}{M}\rho-\frac{1}{12}\frac{k_f^4}{M^3}\rho+C_s^2\frac{\rho^2}{M^2}\frac{1}{2}\frac{k_f^2}{M^2}, \tag{47}$$

$$M^*=M-C_s^2\frac{\rho}{M}\left(1-\frac{1}{4}\frac{k_f^2}{M^2}\right), \tag{48}$$

1D:

$$\frac{\mathcal{E}}{\rho}-M=\left(\frac{C_v^2-C_s^2}{2M^2}\right)\rho+\frac{1}{6}\frac{k_f^2}{M}-\frac{1}{40}\frac{k_f^4}{M^3}+C_s^2\frac{\rho}{M}\frac{1}{6}\frac{k_f^2}{M}, \tag{49}$$

$$p=\left(\frac{C_v^2-C_s^2}{2M^2}\right)\rho^2+\frac{1}{3}\frac{k_f^2}{M}\rho-\frac{1}{10}\frac{k_f^4}{M^3}\rho+C_s^2\frac{\rho^2}{M^2}\frac{1}{2}\frac{k_f^2}{M^2}, \tag{50}$$

$$M^*=M-C_s^2\rho\left(1-\frac{1}{6}\frac{k_f^2}{M^2}\right). \tag{51}$$

This set of equations can be easily solved for C_s^2 and C_v^2 by minimizing the binding energy for $\rho=\rho_0$ and imposing that $B_0=\mathcal{E}/\rho_0-M$ and $p(\rho_0)=0$, where ρ_0 is a given equilibrium density. What is important here is that the first order relativistic correction prevents collapse for all dimensionalities. This occurs because the last term in Eqs. (43), (46), and (49) ensures the positivity of the high density behavior for all cases. However, the saturation point now is restricted to a certain region of B_0 and ρ_0, as we will show in the next section.

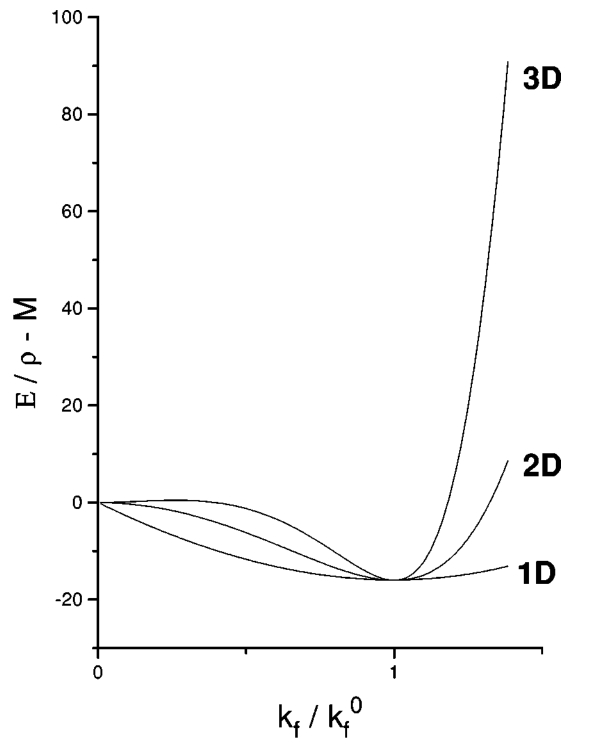

FIG. 1. The energy per particle $\mathcal{E}/\rho-M$ versus k_f/k_f^0. The spatial dimensions are specified besides each curve.

IV. RESULTS AND DISCUSSION

Infinite nuclear matter saturates for a binding energy (the negative of the per-particle energy) $B_0=16$ MeV at the equilibrium density $\rho_0=0.15\ \mathrm{fm}^{-3}$, corresponding to a Fermi momentum $k_f^0=1.3\ \mathrm{fm}^{-1}$. Motivated by this experimental situation, in our applications for the idealized 2D and 1D cases, we will impose that such idealized models saturate for $B_0=16$ MeV at $k_f^0=1.3\ \mathrm{fm}^{-1}$. Hereafter, unless otherwise specified, all tables and figures present the model comparatively for 3D, 2D, and 1D. In Fig. 1 we present the energy per particle $\mathcal{E}/\rho-M$ versus k_f/k_f^0. In Table I, the dimensionless constants C_s^2 and C_v^2 are given, as well as the values for the effective baryonic mass $y=M^*/M$, the compression modulus K, vector potential V, and scalar potential S.

Analyzing the relativistic content of the model as indicated by the effective mass, we are led to the conclusion that, as dimension decreases, the model becomes less relativistic and softer at the saturation point. In order to have a better description of this statement in a broader range of momenta, we show in Fig. 2 the effective mass y versus k_f/k_f^0. Note that at low momenta, the lower the dimension, the lower the effective mass. It is easy to infer from this figure where this behavior changes and where crossovers take place. More conclusive indications of how relativistic the model is can be extracted from ρ_s/ρ versus k_f/k_f^0, presented in Fig. 3.

In order to see how the model approaches the causal limit, we calculated the sound velocity defined by $v_s=\partial p/\partial\mathcal{E}$ plotted against k_f/k_f^0 in Fig. 4. To clarify whether or not the dimensionality of the EOS affects the high density limit of $\mathcal{E}/\rho$, we have calculated this quantity, obtaining $\mathcal{E}/\rho\rightarrow 1$, which shows that the phase space constraint does not affect this limit, meaning that the vector repulsive interaction dominates at high density for all dimensionalities. Following our analysis, we present in the Appendix expansions in terms of k_f for the effective mass, density energy, and pressure, in which we can identify the nonrelativistic terms and the onset of the relativistic effect corrections, appearing gradually with

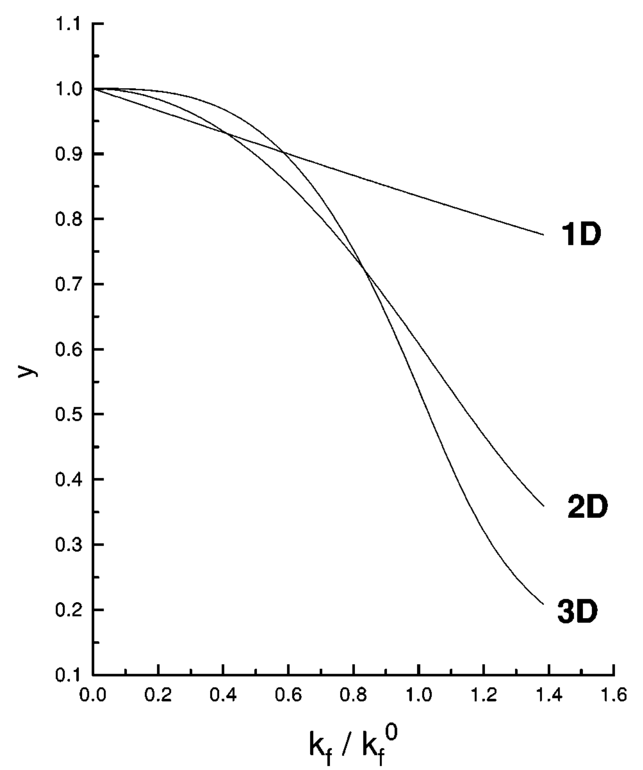

FIG. 2. The effective mass y versus k_f/k_f^0. The spatial dimensions are specified beside each curve.

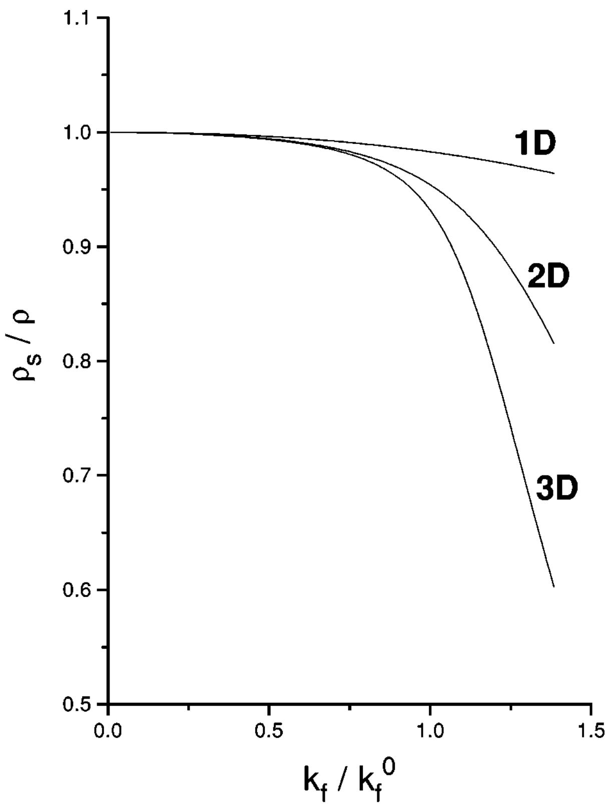

FIG. 3. The ratio between scalar and baryonic densities ρ_s/ρ versus k_f/k_f^0. The spatial dimensions are specified beside each curve.

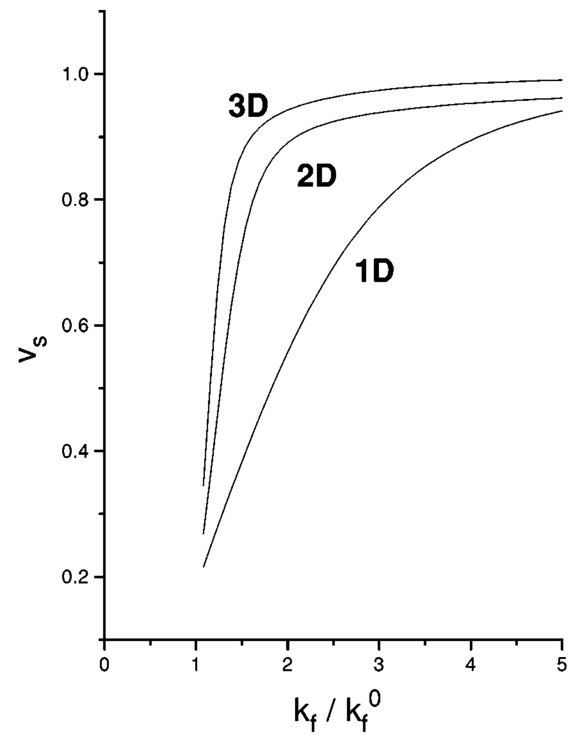

FIG. 4. The sound velocity $v_s = \partial p/\partial \mathcal{E}$ versus k_f/k_f^0 in units of the light velocity. The spatial dimensions are specified beside each curve.

the many-body force terms, in powers of ρ.

The nonrelativistic limit shows that the 1D case saturates. This is consistent with the fact that, from our previous discussion, this is indeed the case where one least needs relativistic effects to bind the system. However, Eq. (41), here rewritten as $k_f = (6MB_0)^{1/2}$, demonstrates the direct relation between the density and the binding energy: once one of them is fixed the other can no longer be freely determined. So, as an example, if we choose $B_0 = 16$ MeV we obtain $k_f = 1.52\ \mathrm{fm}^{-1}$. On the other hand, if we choose to fix $k_f = 1.3\ \mathrm{fm}^{-1}$ then $B_0 = 11.7$ MeV.

The first-order relativistic correction, see Eqs. (43), (46), and (49), is already enough to change this scenario in all dimensionalities, since now saturation is possible. This saturation, however, becomes restricted to a region in the (B_0, k_f) plane as we show in Fig. 5. The crucial reason to restrict the space of solutions is that large values of C_s^2 and C_v^2 are needed to saturate the system, compared to the fully relativistic case. When this happens, Eqs. (45), (48), and (51) start leading to negative unphysical solutions for M^*/M, which obviously have to be discarded, thus restricting the region of physically acceptable saturation. In particular, we stress that the 3D case does not allow saturation at the first order of relativistic expansion for $B_0 = 16$ MeV and $k_f = 1.3\ \mathrm{fm}^{-1}$. From Fig. 5 we see that only the 1D case can obtain saturation at that point. More important here than the saturation point itself is the fact that the first order relativistic correction is enough to avoid the nonrelativistic collapse for 3D and 2D cases.

Still regarding the expansion analysis, and to see how the

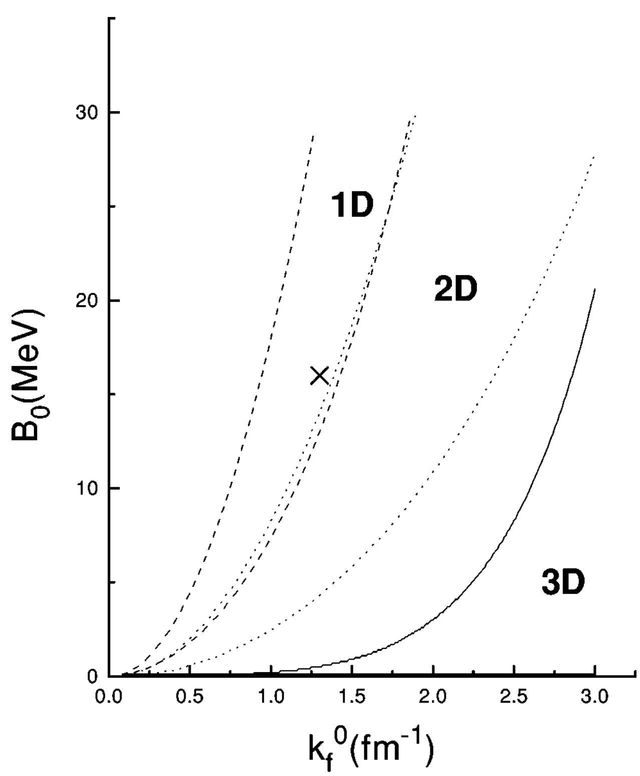

FIG. 5. The (B_0, k_f) plane of saturation solutions for Eqs. (43)–(51). The allowed space of solutions lie within the dashed curves for 1D, the dotted curves for 2D, and the solid curves for 3D. The point X has as coordinates the values for nuclear matter saturation.

TABLE I. Dimensionless constants from fits of nuclear matter equilibrium properties ($B_0 = 16$ MeV, $k_f = 1.3\ \mathrm{fm}^{-1}$). Values are given for the effective baryonic mass M^*/M, the compression modulus K (MeV), vector potential V (MeV), and scalar potential S (MeV).

Model	3D	2D	1D
C_s^2	359.348	17.259	0.483
C_v^2	275.116	13.289	0.301
M^*/M	0.539	0.609	0.835
K	554.322	182.302	36.380
V	355.798	296.444	98.192
S	−433.123	−367.366	−155.099

various relativistic orders contribute to the saturation, we use C_s^2 and C_v^2, given in Table I, obtained in the fully relativistic calculation, to build up higher relativistic orders. Such a result is given in Table II.

V. CONCLUSIONS

We have presented the relativistic Walecka model in the mean field approach for one, two, and three spatial dimensions. Our main conclusions are as follows.

(1) A unified and closed expression for the compression modulus is obtained, as a function only of the dimension D, Eq. (30).

(2) We have shown that the two-dimensional case presents the interesting aspect of having an algebraic analytical solution for the relativistic equation of state. Although the expression is not a simple one, as given fundamentally by Eq. (31), the model may be thought of as exactly solvable for all densities. This fact is auspicious in itself, since it is absolutely not usual for relativistic many-body systems to display analytical solutions, even in the apparently simpler one-dimension models.

(3) Motivated by the 3D case of the model, which simulates well the bulk properties of nuclear matter, we have extended the applications to the idealized 2D and 1D cases. We illustrate in our figures the impact on several quantities, such as energy per particle, compression modulus, pressure, sound velocity, and causal limit, provoked when spatial phase space is restricted. From our results it turns out that the lower the dimensionality, the smaller the relativistic content of the model is (see Fig. 3).

(4) A closed and unified relativistic expansion for the model has been achieved [Eqs. (32)–(34)]. From this expansion we have shown that the relation $(\mathcal{E}+p)/\rho=\mu$ holds, ensuring the consistency of the relativistic expansion with the Hugenholtz-van Hove theorem at each order.

(5) A relativistic expansion of the model showed that (a) the nonrelativistic limit of the model allows saturation solution only in the 1D case but with the impossibility of simultaneously fitting binding energy and equilibrium density [see Eq. (37)]. (b) the first-order relativistic correction restricts the (B_0, k_f) plane solution of the model (see Fig. 5) and in the 3D case, a $B_0 = 16$ MeV for a value of $k_f = 1.3\ \mathrm{fm}^{-1}$ is not possible.

(6) We have depicted the isolated contributions to the binding energy for many orders of the relativistic correction (see Table II). Our results indicate that it is necessary to have very high k_f powers to get the same saturation result as when calculated from the fully relativistic model.

(7) Finally, let us clarify the reason why we have, throughout this paper, always discussed saturation related to the collapse of the system. We are aware that usually the collapse is connected to the zero range of the model (the range limit where the Thomas effect takes place). The question of the collapse of nuclear matter in different space dimensions is important in itself. Notice that the Thomas effect is supposed to occur only for bosons and in 3D. Here we are adding two different elements to the discussion: (a) We have dealt with fermions, and (b) we have treated the system fully relativistically. In what respect can our study be seen as also representing the zero range limit? Let us recall that the Walecka model, when applied to infinite systems (nuclear matter) through the mean-field approach (MFA), reduces the ini-

TABLE II. Isolated nonrelativistic (NR) and relativistic (R) contributions for the binding energy, in MeV, from the expansions for 3D, 2D, and 1D cases with C_s^2 and C_v^2 given by Table I. Each row identifies the k_f order of the term. Values smaller than 10^{-3} are represented by 0. Gaps identify when the particular order is not present. The total contribution is also indicated.

Model	3D		2D		1D	
	NR	R	NR	R	NR	R
$\mathcal{O}(k_f^1)$					−29.798	
$\mathcal{O}(k_f^2)$	21.025		−26.765		11.680	
$\mathcal{O}(k_f^3)$	−54.467					1.963
$\mathcal{O}(k_f^4)$	−0.280		−0.218	7.184	−0.131	0.330
$\mathcal{O}(k_f^5)$		10.406				−0.023
$\mathcal{O}(k_f^6)$	0.008		0.006	2.610	0.003	0.040
$\mathcal{O}(k_f^7)$		−0.533				0
$\mathcal{O}(k_f^8)$	0	5.150	0	0.543	0	0
$\mathcal{O}(k_f^9)$		0.029				0
$\mathcal{O}(k_f^{10})$	0	−0.642	0	−0.145	0	0
$\mathcal{O}(k_f^{11})$		2.547				0
Partials	−33.715	16.957	−26.977	10.192	−18.245	2.310
Totals	−16.758		−16.784		−15.935	

tial number of four free parameters (scalar and vector masses and coupling constants) to only two, $C_s^2 = g_s^2 M^{D-1}/m_s^2$ and $C_v^2 = g_v^2 M^{D-1}/m_v^2$. This means that, in principle, the mesonic masses could be thought of as being as large as possible, as long as the corresponding mesonic coupling constants were also large enough to keep the values of C_s^2 and C_v^2 fixed. Now let us stress the fact that the MFA itself acquires validity as the system's density increases, which is precisely where collapse takes place. Based on the above arguments we conclude this work by conjecturing for short-ranged many-body fermionic systems (in this point we are abandoning the specific aspects of nuclear matter itself) the following. (a) Relativistic effects together with the Pauli principle tend to prevent collapse. (b) In the 1D case, the Pauli principle by itself is enough to prevent the collapse, since the Fermi kinetic energy ensures the saturation of the system. (c) 2D and 3D cases need a relativistic description to attain saturation of the many-body system.

ACKNOWLEDGMENTS

The authors would like to express their thanks to Conselho Nacional de Desenvolvimento Científico e Tecnológico (CNPq) for partial financial support.

APPENDIX

In this appendix, we present the relativistic expansion for the models. We start by performing a M^* expansion in powers of k_f iteratively in Eq. (32). Afterwards we use this expansion in Eqs. (33), (34). The results are given, specifying each dimensional case.

3D:

$$M^* = M - \left(\frac{g_s}{m_s}\right)^2 \rho \left\{ 1 - \frac{3}{10}\left(\frac{k_f}{M}\right)^2 + \frac{9}{56}\left(\frac{k_f}{M}\right)^4 - \frac{5}{48}\left(\frac{k_f}{M}\right)^6 + \frac{105}{1408}\left(\frac{k_f}{M}\right)^8 - \left(\frac{g_s}{m_s}\right)^2 \frac{\rho}{M}\left[\frac{3}{5}\left(\frac{k_f}{M}\right)^2 - \frac{144}{175}\left(\frac{k_f}{M}\right)^4\right] - \left(\frac{g_s}{m_s}\right)^4 \rho^2 \frac{9}{10}\frac{k_f^2}{M^4}\right\}, \tag{A1}$$

$$\frac{\mathcal{E}}{\rho} - M = \frac{3}{10}\frac{k_f^2}{M} + \frac{1}{2}\left[\left(\frac{g_v}{m_v}\right)^2 - \left(\frac{g_s}{m_s}\right)^2\right]\rho + \left[-\frac{3}{56}\frac{k_f^4}{M^3} + \frac{1}{48}\frac{k_f^6}{M^5} - \frac{15}{1408}\frac{k_f^8}{M^7} + \frac{21}{3328}\frac{k_f^{10}}{M^9} + \cdots\right] + \left(\frac{g_s}{m_s}\right)^2 \frac{\rho}{M}\left[\frac{3}{10}\frac{k_f^2}{M} - \frac{36}{175}\frac{k_f^4}{M^3} + \frac{16}{105}\frac{k_f^6}{M^5} - \frac{64}{539}\frac{k_f^8}{M^7} + \cdots\right] + \left[\left(\frac{g_s}{m_s}\right)^2 \frac{\rho}{M}\right]^2 \left[\frac{3}{10}\frac{k_f^2}{M} - \frac{351}{700}\frac{k_f^4}{M^3} + \cdots\right] + \left[\left(\frac{g_s}{m_s}\right)^2 \frac{\rho}{M}\right]^3 \left[\frac{3}{10}\frac{k_f^2}{M} + \cdots\right], \tag{A2}$$

$$p = \frac{1}{2}\left[\left(\frac{g_v}{m_v}\right)^2 - \left(\frac{g_s}{m_s}\right)^2\right]\rho^2 + \rho\left[\frac{1}{5}\frac{k_f^2}{M} - \frac{1}{14}\frac{k_f^4}{M^3} + \frac{1}{24}\frac{k_f^6}{M^5} - \frac{5}{176}\frac{k_f^8}{M^7} + \frac{35}{1664}\frac{k_f^{10}}{M^9} + \cdots\right] + \left(\frac{g_s}{m_s}\right)^2 \rho^2 \left[\frac{1}{2}\left(\frac{k_f}{M}\right)^2 - \frac{12}{25}\left(\frac{k_f}{M}\right)^4 + \frac{17}{40}\left(\frac{k_f}{M}\right)^6 - \frac{64}{147}\left(\frac{k_f}{M}\right)^8 + \cdots\right] + \left(\frac{g_s}{m_s}\right)^4 \rho^3 \left[\frac{4}{5}\frac{k_f^2}{M^3} - \frac{51}{35}\frac{k_f^4}{M^5} + \cdots\right] + \left(\frac{g_s}{m_s}\right)^6 \rho^4 \left[\frac{11}{10}\frac{k_f^2}{M^4} + \cdots\right]; \tag{A3}$$

2D:

$$M^* = M - \left(\frac{g_s}{m_s}\right)^2 \rho \left\{ 1 - \frac{1}{4}\left(\frac{k_f}{M}\right)^2 + \frac{1}{8}\left(\frac{k_f}{M}\right)^4 - \frac{5}{64}\left(\frac{k_f}{M}\right)^6 + \frac{7}{128}\left(\frac{k_f}{M}\right)^8 - \left(\frac{g_s}{m_s}\right)^2 \frac{\rho}{M}\left[\frac{1}{2}\left(\frac{k_f}{M}\right)^2 - \frac{5}{8}\left(\frac{k_f}{M}\right)^4 + \frac{21}{32}\left(\frac{k_f}{M}\right)^6\right] - \left(\frac{g_s}{m_s}\right)^4 \left(\frac{\rho}{M}\right)^2 \left[\frac{3}{4}\left(\frac{k_f}{M}\right)^2 - \frac{27}{16}\left(\frac{k_f}{M}\right)^4\right]\right\}, \tag{A4}$$

$$\frac{\mathcal{E}}{\rho} - M = \frac{1}{4}\frac{k_f^2}{M} + \frac{1}{2}\left[\left(\frac{g_v}{m_v}\right)^2 - \left(\frac{g_s}{m_s}\right)^2\right]\rho + \left[-\frac{1}{24}\frac{k_f^4}{M^3} + \frac{1}{64}\frac{k_f^6}{M^5} - \frac{1}{128}\frac{k_f^8}{M^7} + \frac{7}{1536}\frac{k_f^{10}}{M^9} + \cdots\right] + \left(\frac{g_s}{m_s}\right)^2 \frac{\rho}{M}\left[\frac{1}{4}\frac{k_f^2}{M} - \frac{5}{32}\frac{k_f^4}{M^3} + \frac{7}{64}\frac{k_f^6}{M^5} - \frac{21}{256}\frac{k_f^8}{M^7} + \cdots\right] + \left[\left(\frac{g_s}{m_s}\right)^2 \frac{\rho}{M}\right]^2 \left[\frac{1}{4}\frac{k_f^2}{M} - \frac{3}{8}\frac{k_f^4}{M^3} + \frac{7}{16}\frac{k_f^6}{M^5} + \cdots\right] + \left[\left(\frac{g_s}{m_s}\right)^2 \frac{\rho}{M}\right]^3 \left[\frac{1}{4}\frac{k_f^2}{M} - \frac{23}{48}\frac{k_f^4}{M^3} + \cdots\right], \tag{A5}$$

$$p = \frac{1}{2}\left[\left(\frac{g_v}{m_v}\right)^2 - \left(\frac{g_s}{m_s}\right)^2\right]\rho^2 + \rho\left[\frac{1}{4}\frac{k_f^2}{M} - \frac{1}{12}\frac{k_f^4}{M^3} + \frac{3}{64}\frac{k_f^6}{M^5} - \frac{1}{32}\frac{k_f^8}{M^7} + \frac{35}{1536}\frac{k_f^{10}}{M^9} + \cdots\right] + \left(\frac{g_s}{m_s}\right)^2 \rho^2 \left[\frac{1}{2}\left(\frac{k_f}{M}\right)^2 - \frac{15}{32}\left(\frac{k_f}{M}\right)^4 + \frac{7}{16}\left(\frac{k_f}{M}\right)^6 - \frac{105}{256}\left(\frac{k_f}{M}\right)^8 + \cdots\right] + \left(\frac{g_s}{m_s}\right)^4 \rho^3 \left[\frac{3}{4}\frac{k_f^2}{M^3} - \frac{3}{2}\frac{k_f^4}{M^5} + \frac{35}{16}\frac{k_f^6}{M^7} + \cdots\right] + \left(\frac{g_s}{m_s}\right)^6 \rho^4 \left[\frac{k_f^2}{M^4} - \frac{157}{48}\frac{k_f^4}{M^6} + \cdots\right]; \tag{A6}$$

1D:

$$M^* = M - \left(\frac{g_s}{m_s}\right)^2 \rho \Bigg\{ 1 - \frac{1}{6}\left(\frac{k_f}{M}\right)^2 + \frac{3}{40}\left(\frac{k_f}{M}\right)^4 - \frac{5}{12}\left(\frac{k_f}{M}\right)^6 - \left(\frac{g_s}{m_s}\right)^2 \frac{\rho}{M}\left[\frac{1}{3}\left(\frac{k_f}{M}\right)^2 - \frac{16}{45}\left(\frac{k_f}{M}\right)^4 + \frac{12}{35}\left(\frac{k_f}{M}\right)^6\right]$$
$$- \left(\frac{g_s}{m_s}\right)^4 \left(\frac{\rho}{M}\right)^2 \left[\frac{1}{2}\left(\frac{k_f}{M}\right)^2 - \frac{37}{36}\left(\frac{k_f}{M}\right)^4\right] - \left(\frac{g_s}{m_s}\right)^6 \left(\frac{\rho}{M}\right)^3 \left[\frac{2}{3}\left(\frac{k_f}{M}\right)^2 - \frac{7}{6}\left(\frac{k_f}{M}\right)^4\right] - \left(\frac{g_s}{m_s}\right)^8 \left(\frac{\rho}{M}\right)^4 \left[\frac{5}{6}\left(\frac{k_f}{M}\right)^2\right]$$
$$- \left(\frac{g_s}{m_s}\right)^{10} \left(\frac{\rho}{M}\right)^5 \left[\frac{5}{6}\left(\frac{k_f}{M}\right)^2\right]\Bigg\}, \tag{A7}$$

$$\frac{\mathcal{E}}{\rho} - M = \frac{1}{6}\frac{k_f^2}{M} + \frac{1}{2}\left[\left(\frac{g_v}{m_v}\right)^2 - \left(\frac{g_s}{m_s}\right)^2\right]\rho + \left[-\frac{1}{40}\frac{k_f^4}{M^3} + \frac{1}{112}\frac{k_f^6}{M^5} - \frac{5}{1152}\frac{k_f^8}{M^7} + \cdots\right] + \left(\frac{g_s}{m_s}\right)^2 \frac{\rho}{M}\left[\frac{1}{6}\frac{k_f^2}{M} - \frac{4}{45}\frac{k_f^4}{M^3} + \frac{2}{35}\frac{k_f^6}{M^5} + \cdots\right]$$
$$+ \left[\left(\frac{g_s}{m_s}\right)^2 \frac{\rho}{M}\right]^2 \left[\frac{1}{6}\frac{k_f^2}{M} - \frac{37}{180}\frac{k_f^4}{M^3} + \cdots\right] + \left[\left(\frac{g_s}{m_s}\right)^2 \frac{\rho}{M}\right]^3 \left[\frac{1}{6}\frac{k_f^2}{M} - \frac{7}{18}\frac{k_f^4}{M^3} + \cdots\right] + \left[\left(\frac{g_s}{m_s}\right)^2 \frac{\rho}{M}\right]^4 \left[\frac{1}{6}\frac{k_f^2}{M} + \cdots\right]$$
$$- \left[\left(\frac{g_s}{m_s}\right)^2 \frac{\rho}{M}\right]^5 \left[\frac{2}{3}\frac{k_f^2}{M} + \cdots\right] - \left[\left(\frac{g_s}{m_s}\right)^2 \frac{\rho}{M}\right]^6 \left[\frac{2}{3}\frac{k_f^2}{M} + \cdots\right], \tag{A8}$$

$$p = \frac{1}{2}\left[\left(\frac{g_v}{m_v}\right)^2 - \left(\frac{g_s}{m_s}\right)^2\right]\rho^2 + \rho\left[\frac{1}{3}\frac{k_f^2}{M} - \frac{1}{10}\frac{k_f^4}{M^3} + \frac{3}{56}\frac{k_f^6}{M^5} - \frac{5}{144}\frac{k_f^8}{M^7} + \cdots\right] + \left(\frac{g_s}{m_s}\right)^2 \rho^2 \left[\frac{1}{2}\left(\frac{k_f}{M}\right)^2 - \frac{4}{9}\left(\frac{k_f}{M}\right)^4 + \frac{21}{40}\left(\frac{k_f}{M}\right)^6 + \cdots\right]$$
$$+ \left(\frac{g_s}{m_s}\right)^4 \rho^3 \left[\frac{2}{3}\frac{k_f^2}{M^3} - \frac{37}{90}\frac{k_f^4}{M^5} + \cdots\right] + \left(\frac{g_s}{m_s}\right)^6 \rho^4 \left[\frac{5}{6}\frac{k_f^2}{M^4} - \frac{49}{18}\frac{k_f^4}{M^6} + \cdots\right] + \left(\frac{g_s}{m_s}\right)^8 \rho^5 \left[\frac{5}{6}\frac{k_f^2}{M^5} + \cdots\right] + \left(\frac{g_s}{m_s}\right)^{10} \rho^6 \left[\frac{7}{6}\frac{k_f^2}{M^6} + \cdots\right]$$
$$+ \left(\frac{g_s}{m_s}\right)^{12} \rho^7 \left[\frac{7}{6}\frac{k_f^2}{M^7} + \cdots\right]. \tag{A9}$$

[1] J. MaGuire, J. Math. Phys. **6**, 432 (1965).

[2] F. Calogero and A. Degasperis, Phys. Rev. A **11**, 265 (1975).

[3] D. Campbell, in *Nuclear Physics with Heavy Ions and Mesons*, edited by R. Balian, M. Rho, and G. Ripka, Les Houches Summer School XXX (North-Holland, Amsterdam 1978), Vol. 2, p. 673.

[4] J. W. Negele, Rev. Mod. Phys. **54**, 913 (1982).

[5] L. H. Thomas, Phys. Rev. **47**, 903 (1935).

[6] V. Efimov, Phys. Lett. **33B**, 563 (1970).

[7] S. K. Adhikari, A. Delfino, T. Frederico, I. D. Goldman, and L Tomio, Phys. Rev. A **37**, 3666 (1988); S. K. Adhikari, A. Delfino, T. Frederico, and L. Tomio, *ibid.* **47**, 1093 (1993).

[8] T. Frederico, Phys. Lett. B **282**, 409 (1992).

[9] M. E. Bracco, F. S. Navarra, and M. C. Nemes, Physica A **203**, 671 (1994).

[10] A. J. Buchmann, A. Faessler, and M. I. Krivoruchenko, Ann. Phys. (N.Y.) **254**, 109 (1997).

[11] B. D. Serot, S. E. Koonin, and J. W. Negele, Phys. Rev. C **28**, 1679 (1983).

[12] J. D. Walecka, Ann. Phys. (N.Y.) **83**, 491 (1974); B. D. Serot and J. D. Walecka, *Advances in Nuclear Physics* (Plenum, New York, 1986), Vol. 16, pp. 1–327; R. J. Furnstahl and B. D. Serot, Phys. Rev. C **41**, 262 (1990).

[13] J. L. Forest and V. R. Pandharipande, Phys. Rev. C **52**, 568 (1995).

[14] C. Speicher, E. Engel, and R. M. Dreizler, Nucl. Phys. **A562**, 569 (1993).

[15] J. P. Blaizot, Phys. Rep. **64**, 174 (1980).

[16] N. M. Hugenholtz and L. Van Hove, Physica (Amsterdam) **24**, 363 (1958).

[17] J. Boguta, Phys. Lett. **106B**, 250 (1981).